

Article

Not peer-reviewed version

Analysis of Inclusions and Impurities Present in Typical HpdC, Stamping and Extrusion Alloys Produced with Different Scrap Levels

[Manel Da Silva](#)*, [Jaume Pujante](#), [Joanna Hrabia-Wisnios](#), [Boguslaw Augustyn](#), [Dawid Kapinos](#), [Mateusz Węgrzyn](#), [Sonia Boczkal](#)

Posted Date: 11 April 2024

doi: 10.20944/preprints202404.0783.v1

Keywords: aluminium alloys; recycling; impurities; flowability; casting



Preprints.org is a free multidiscipline platform providing preprint service that is dedicated to making early versions of research outputs permanently available and citable. Preprints posted at Preprints.org appear in Web of Science, Crossref, Google Scholar, Scilit, Europe PMC.

Copyright: This is an open access article distributed under the Creative Commons Attribution License which permits unrestricted use, distribution, and reproduction in any medium, provided the original work is properly cited.

Article

Analysis of Inclusions and Impurities Present in Typical HPDC, Stamping and Extrusion Alloys Produced with Different Scrap Levels

Manel da Silva ^{1,*}, Jaume Pujante ¹, Joanna Hrabia-Wiśnios ², Bogusław Augustyn ², Dawid Kapinos ², Mateusz Węgrzyn ² and Sonia Boczkal ²

¹ Eurecat, Centre Tecnològic de Catalunya. Unit of Metallic and Ceramic Materials, Avda. Universitat Autònoma 23, Cerdanyola del Vallès, 08290, Spain; info@eurecat.org

² Lukaszewicz Research Network – Institute of Non Ferrous Metals, Light Metals Centre, Pilsudski 19 street, 32-050 Skawina, Poland

* Correspondence: manel.dasilva@eurecat.org

Abstract: The European Green Deal poses a two-pronged challenge for the automotive industry: migrating to solutions based in light structures, requiring light weight concepts and light materials, while at the same time avoiding dependence towards the importation of these advanced materials. Aluminium alloys are lightweight and cost-effective materials that can successfully cover the requirements of many structural applications, however their production requires from bauxite and other Critical Raw Materials (CRM), such as Si and Mg. Aluminium alloys are fully recyclable, but scrap is usually contaminated and its use is related to an increment of impurities, tramp element and undesired inclusions. Traditionally, the use of secondary alloys has been restricted to low performance applications. The present work analyses the effect that the use of scrap has in the quantity of inclusions present in the alloy and in other properties relevant for the material processing. The study was carried out for common alloys belonging to 3 of the most common aluminium processes used in the car manufacturing industry: High Pressure Die Casting (HPDC) (EN AC-43500), extrusion (6063) and sheet metal forming (5754 and 6181). Reference alloy were mixed with different level of scrap (0, 20, 40, 60, 80 and 100%) trying to keep the chemical composition as unaffected as possible. The inclusions level of the alloy was characterized with the Prefil Footprinter® test. In addition, the obtained materials, after being cast in an open mould, were subjected to metallographic characterization. Relevant properties to assess the formability quality of the alloys for the corresponding transforming process, were obtained: flowability test for HPDC alloy and high temperature compression for extrusion alloys. The results obtained suggest that the number of inclusions present in the melt highly increase with the amount of scrap used to produce the alloy. These inclusions are also related with an important lost of flowability, but do not have a noticeable impact on microstructure.

Keywords: aluminium alloys; recycling; impurities; flowability; casting

1. Introduction

The European Green Deal poses a two-pronged challenge for the automotive industry: migrating to solutions based in light structures, requiring light weight concepts and light materials, while at the same time avoiding dependence towards the importation of these advanced materials.

Aluminium is a lightweight and cost-effective material, that can successfully cover the requirements of many structural applications. The use of aluminium in vehicles has been steadily growing over the last decades [1], substituting steel and cast iron and making vehicles more efficient and less fuel demanding [2]. As a reference, weight reduction potential of up to 20-30% was estimated by making use of high-performance aluminium grades when compared to traditional steel-based

construction [3]. However, these high-performance parts need to be produced in primary aluminium alloys requiring bauxite, as well as other alloying elements classified as sensitive by the CRM alliance, the most common of those being metallic Silicon (Si) and Magnesium (Mg).

While aluminium recycling is spread in the automotive industry, recycled alloys are currently not able to fulfil the properties required by structural applications due to limitations in their formability and mechanical performance. As a reference, a study from 2011 quantified in one third the amount of scrap used in the making of high-performance aluminium alloys [4]. Moreover, the parts traditionally produced with intensive use of recycled aluminium (motor blocks, gear boxes, oil pans, valve covers) [5] are not present in electrical vehicles. Therefore, a better understanding of the how scrap affects aluminium properties is required, in order to develop new high performance, environmentally and strategically sustainable aluminium grades and their forming processes, is fundamental for sustainable electrification of the automotive industry.

The assessment of the purity of aluminium alloys is critical for both quality and process control and is defined by the number of inclusions (native and/or exogenous particles) present in the molten metal [6,7]. Depending on the size and proportion of inclusions, i.e., single large inclusions or a large number of small inclusions, these can have a negative effect on the mechanical and chemical properties of the final product.

For cast products, in order to be able to produce the highest possible quality aluminium alloy, liquid metal preparation processes are carried out first [8,9]. These processes require effective purification and refining procedures, for which salt additives are used and refining is carried out by degassing [6,8–11].

In the case of wrought products, material improvement needs to be done during the production of the intermediate format; e.g., hot rolling for a sheet metal grade, extrusion of a cast ingot through a die or shaping a bulk material through hot forging. All these hot forming processes change the cast microstructure into a more homogeneous and textured recrystallized morphology; correcting segregation while at the same time fragmenting inclusions and closing small voids. Despite these measures, the impurity content still affects the mechanical properties of the material. In the particular case of sheet metal, intermetallic particles can be detrimental to the formability of the alloy, as discussed for instance in references [7,12].

On the other hand, alternative processing strategies exist for high purity alloys, such as filtration. In this case, the casting process is carried out by pouring the liquid metal through appropriately selected ceramic filters [6,10]. By using this procedure, a significant amount of solid inclusions are entrapped in the filter and do not reach the product. This process can also be used as an analytical device to characterize the inclusion profile in an alloy; work in this paper has used this technique.

Great deal of research has already been done on the subject of inclusion analysis, which has led to a division into the main groups of impurities: oxide films, carbides, magnesium oxides, refractory materials, metal treatments, others, and additives [10]. In the case of casting alloys, it has been shown that oxide films in solid aluminium alloys are formed by the entrainment of the surface of the metal in the liquid state. The oxide layers act as substrates for the precipitation of other phases on their wetted external surfaces. Oxides observed in Al-11.5Si-0.4Mg casting alloys include Al_2MgO_4 , Al_2O_3 and MgO. Oxide is one of the most deleterious and pervasive inclusion types in Al-Mg melts. They are generally formed by oxidative reactions due to high oxygen affinity of aluminium and magnesium. In Al-Mg alloys, the tendency to oxidize increases rapidly with increasing Mg content. The oxidation reaction path depends on the amount of Mg and probably starts with the formation of amorphous MgO, MgAl_2O_4 or Al_2O_3 , which then transforms into crystalline MgO, MgAl_2O_4 or $\gamma\text{-Al}_2\text{O}_3$ films. The high concentration of Mg on the alloy surface promotes initial oxidation to MgO. Moreover, since MgAl_2O_4 is more thermodynamically stable than MgO, MgO gives way to MgAl_2O_4 with longer reaction times [13,14]. The MgAl_2O_4 spinels are the most detrimental inclusions in aluminium because of their large size and hardness. Spinel Al_2MgO_4 is the main type in the experimental alloys, mainly due to its magnesium content. Aluminium oxide Al_2O_3 is formed either under conditions of local magnesium depletion or is derived from the feedstock. The MgO film can

come from the original ingots. SiO₂ inclusions are trapped either in the sand or in the refractory material and are themselves surrounded by an oxide film [15].

These oxide layers and inclusions are also present in wrought alloys. Samples of AA5038 alloys taken in the Wagstaff plant at a temperature of 680-690°C show Al₂O₃ content, which may originate from the electrolysis raw material (aluminium oxide not dissolved in the salt bath), or from the refractory filter or from the casting ladle. Spherical agglomerates of magnesium and aluminium silicate and TiB₂ particles formed from AlTi₅B₁ mortars were observed at the interface between the ceramic filter and the 5038 alloy [9,16].

Microscopic analysis of the inclusions above the filter as well as the billet samples showed the presence of magnesium oxides and spinels due to the Mg content of 0.4 to 0.55% in the 6063 alloys. In addition to the dominant oxides, TiB₂ and Al₄C₃ inclusions have also been observed. The carbides are formed during the reduction of the pot cells in the aluminium smelting process. Al₄C₃ <3 µm inclusions are not considered harmful. TiB₂ agglomerates were present in significant amounts and formed as a result of the addition of the AlTi₅B₁ grain refiner to the melt. For alloys purified by SNIF degassing, it has been shown that oxides greater than 50 µm and borides greater than 20 µm are removed while smaller borides agglomerate [6].

The chemical reactivity leading to the formation of impurities, their decomposition and size is mainly due to small changes in the chemical composition of the alloy and the conditions under which the process of preparing the liquid metal for casting is carried out [6,17]. Therefore, in the current research to achieve a zero waste effect, it becomes extremely valuable to know how to remelt scrap with maximum contribution.

This paper presents an analysis of the effect of increasing scrap content on the microstructure and formability on alloys for HDPC, sheet metal and extrusion processes. A Prefil Footprinter® was used to control the level of impurities by assessing the liquid metal flow rate and the type and size of impurities appearing in the microstructure as a function of the scrap content. Specific performance tests were employed on the different materials, including flowability for HPDC, hot compression ductility for extrusion alloys and microstructural evolution for sheet metal.

2. Materials and Methods

2.1. Materials

2.1.1. Aluminium Alloys

Alloys corresponding to three different production processes were analysed: EN AB-43500 for High Pressure Die Casting (HPDC), 6063 for Extrusion, and finally age hardening 6181A and strain hardening 5754 for sheet metal. The aim of this choice was to select representative examples of the major types of aluminium used in passenger automobiles. Chemical composition of the source materials used in this work is shown in Table 1.

Table 1. Average chemical composition (wt.%) of the alloys used in this work determined by mass spectrometry.

n=5	Si	Fe	Cu	Mn	Mg	Zn	Cr	Ni	Pb	Sn	Ti
EN AB-43500	10.40	0.16	0.03	0.65	0.18	<0.01	<0.01	<0.01	<0.01	<0.01	0.07
6063	0.58	0.2	<0.03	0.03	0.48		<0.03	<0.03		<0.03	
6181A	0.91	0.027	0.14	0.3	0.76	0.06	0.02	<0.03	<0.03	<0.03	<0.03
5754	0.14	0.16	0.02	0.16	2.86	<0.03	<0.03	<0.03	<0.03	<0.03	<0.03

2.1.2. Scrap

In order to obtain different levels of recycling, base materials were increasingly mixed with scrap from similar alloys. This procedure will be described in Section 2.2. Scrap was sorted based on morphology and aspect. Sorting methodologies proposed will be described in a specific article in the future.

For die casting, scrap consisted in typical die cast parts; chemical analysis was performed on selected examples, and average values are reported in Table 2 as "Die Casting scrap".

Table 2. Average chemical composition (wt.%) of scrap used in this work as determined by mass spectrometry.

n=5	Si	Fe	Cu	Mn	Mg	Zn	Cr	Ni	Pb	Sn	Ti
Die Casting scrap	10.81	0.15	0.01	0.62	0.26	0.01	<0.01	<0.01	<0.01	<0.01	0.07
"6XXX" scrap	0.45	0.23	0.01	0.04	0.43	0.01	<0.01	<0.01	<0.01	<0.01	0.02

For extrusion and sheet metal materials, the reference alloy was mixed with selected scrap initially identified as 6xxx series fragments, even though in detailed inspection some could be visually residual identified of 5xxx and even 3xxx series. An analysis of the scrap composition was done by measuring 10 different 6XXX series scrap fragments. The average chemical composition of the scrap is presented in Table 2.

2.2. Sample Production

For each alloy, specimens were produced for material characterization with different level of scrap: 0, 20, 40, 60, 80 and 100%. In order to combine several of these tests in one single trial journey, was used the approach of starting with 100% of reference alloy or 100% of scrap and adding the other component, first to a concentration of 20% and in a second step to a concentration of 40%.

2.2.1. HPDC

For the tests with the HPDC alloys, the furnace was charged with about 24,4 kg of one of the materials, either ingot of AlSi10MnMg alloy or of scrap and heated up to a temperature of 710 ± 10 °C.

Scrap was sequentially added, the composition of the different mixtures investigated is presented in Table 3. From the results obtained for the 100% scrap, it can be inferred that the average composition obtained from the measured scrap is in line with the actual average composition of the scrap and most of the scrap belongs to EN AB-43500 alloy.

Table 3. Average chemical composition (wt.%) determined by mass spectrometry of samples taken from the different batch produced from EN AB-43500 alloy.

n=5	Si	Fe	Cu	Mn	Mg	Zn	Cr	Ni	Pb	Sn	Ti
0% scrap	10.34	0.17	0.03	0.58	0.18	<0.03	<0.03	<0.03	<0.01	<0.01	0.06
20% scrap	10.29	0.16	0.02	0.58	0.18	<0.03	<0.03	<0.03	<0.01	<0.01	0.06
40% scrap	10.25	0.16	0.02	0.56	0.19	<0.03	<0.03	<0.03	<0.01	<0.01	0.06
60% scrap	10.1	0.16	0.03	0.53	0.21	<0.03	<0.03	<0.03	<0.01	<0.01	0.06
80% scrap	10.22	0.17	0.03	0.54	0.23	<0.03	<0.03	<0.03	<0.01	<0.01	0.06
100% scrap	10.01	0.14	0.03	0.51	0.25	<0.03	<0.03	<0.03	<0.01	<0.01	0.06
EN AB-43500	9-11.5	<0.20	<0.03	0.4-0.8	0.15-0.6	<0.07	<0.05	<0.05	<0.05	<0.05	<0.15

Three different sample types were casted from the melt: 3 square plates, 3 small ingots and 1 flowability test specimen (Figure 1). These plates (150x150 mm) were filled up to about 25 mm and were used to measure the chemical composition of the batch and to observe the alloy microstructure.



Figure 1. Images of the different sample taken for the tests: square plate (left), small ingot (middle) and flowability test specimen (right).

2.2.2. Extrusion Alloy: 6063

The base material used were 6063 alloy extrusion billets produced by the company ASAS (Table 1); the reference alloy was mixed in different proportions with selected “6XXX-scrap” (Table 2).

A similar procedure as described for HPDC tests was carried out. About 24,4 kg were charged into the furnace, additions of either scrap or billet were introduced into the melt to modify the proportion of feedstock materials used. 3 square plates and 3 small ingots (Figure 1) were casted in each step and were used to characterize the alloys with Prefil Footprinter®, tensile test and optical microscopy, following the same procedure described for HPDC. The chemical composition measured by spectrometry from one of the plates for each batch produced is presented in Table 4.

Table 4. Average chemical composition (wt.%) determined by mass spectrometry of samples taken from the different batch produced from 6063 alloy.

n=5	Si	Fe	Cu	Mn	Mg	Zn	Cr	Ni	Pb	Sn	Ti
0% scrap	0.8	0.2	0.02	0.05	0.48	<0.03	<0.03	<0.03	<0.03	<0.03	<0.03
20% scrap	0.72	0.21	0.02	0.05	0.47	<0.03	<0.03	<0.03	<0.03	<0.03	<0.03
40% scrap	0.62	0.21	0.02	0.05	0.47	<0.03	<0.03	<0.03	<0.03	<0.03	<0.03
60% scrap	0.51	0.23	0.01	0.05	0.45	<0.03	<0.03	<0.03	<0.03	<0.03	<0.03
80% scrap	0.51	0.23	0.02	0.06	0.45	<0.03	<0.03	<0.03	<0.03	<0.03	<0.03
100% scrap	0.5	0.23	0.02	0.06	0.43	<0.03	<0.03	<0.03	<0.03	<0.03	<0.03

2.2.3. Sheet Metal Alloys 6181A and 5754

The company Profilglass supplied commercial 6181A alloy sheets, 2 mm thick, cut in 900 mm x 500 mm blanks. Chemical composition, as determined through spectroscopy, is reported in Table 1. The blanks Among were melted in the furnace mixed with different proportion of “6XXX scrap” (Table 2). The content of Si and Mg was corrected with the addition of master alloys of the corresponding elements. The chemical composition obtained for each batch is presented in Table 5.

Table 5. Average chemical composition (wt.%) determined by mass spectrometry of samples taken from the different batch produced from 6181A alloy.

N=5	Si	Fe	Cu	Mn	Mg	Zn	Cr	Ni	Pb	Sn	Ti
0% scrap	0.88	0.32	0.13	0.29	0.74	0.06	<0.03	<0.03	<0.03	<0.03	<0.03
20% scrap	0.92	0.33	0.11	0.25	0.76	0.08	<0.03	<0.03	<0.03	<0.03	<0.03
40% scrap	0.95	0.32	0.10	0.22	0.71	0.08	<0.03	<0.03	<0.03	<0.03	<0.03
60% scrap	0.96	0.29	0.06	0.14	0.68	0.08	<0.03	<0.03	<0.03	<0.03	<0.03
80% scrap	1.00	0.27	0.05	0.10	0.66	0.08	<0.03	<0.03	<0.03	<0.03	<0.03
100% scrap	1.07	0.26	0.03	0.06	0.65	0.08	<0.03	<0.03	<0.03	<0.03	<0.03

For 6181 (Table 5), the main alloying elements fall within acceptable limits inside the whole range of trials, with some observations. Iron is kept fairly low, mainly due to the carefully selected

scrap; in fact, the level of Fe decreases as scrap rate is increased. This behaviour is not expected to be representative of a scaled-up case of circularity in the current industrial environment, as seen in reference [12]. Manganese was the other elements flagged as conflictive as the used scrap may include 3XXX-series profiles. Manganese turned out to not be an issue due to the scrap selection. Finally, Zn and trace elements Cr and Ti did not significantly worsen through the experiment.

As per desired alloying elements, Silicon and Magnesium were already present in the scrap mix, and additions were calculated considering the average contribution presented in Table 2. Amounts were slightly miscalculated, resulting in an increase in Si content, but it was within the acceptable range of the alloy. Magnesium, on the other hand, was expected to be partially recovered from scrap in the mix. Unfortunately, this contribution was overestimated, and resulted in decreased alloying content through the experiment. It is believed that part of this Mg difference may have oxidated into the dross.

In the case of 5754 alloy, the base material was again commercial 5754 blanks 2 mm thick, 900 mm x 500 mm in size; chemical composition is presented in the first row of Table 6. As in the previous experiments, this material was mixed with scrap that had been identified as 5XXX sheet rests in increasing amounts. In this case, it is noteworthy that the selected scrap appeared to include some fragments of 6XXX alloy.

As a result of this mixture, the chemical composition (Table 6) did not remain as stable as in 6XXX; the value of Silicon in particular experiences significant drift and falls out of specification already at 40% scrap level. Fe, Cu and Mn however are kept in the acceptable range of the alloy, as the 5754 standard tolerates relatively high levels of these elements.

Table 6. Average chemical composition (wt.%) determined by mass spectrometry of samples taken from the different batch produced from 5754 alloy.

n=5	Si	Fe	Cu	Mn	Mg	Zn	Cr	Ni	Pb	Sn	Ti
0% scrap	0.18	0.29	0.02	0.16	2.78	<0.03	<0.03	<0.03	<0.03	<0.03	<0.03
20% scrap	0.23	0.28	0.03	0.18	2.72	<0.03	<0.03	<0.03	<0.03	<0.03	<0.03
40% scrap	0.25	0.26	0.04	0.19	2.66	<0.03	<0.03	<0.03	<0.03	<0.03	<0.03
60% scrap	0.35	0.28	0.06	0.21	2.49	<0.03	<0.03	<0.03	<0.03	<0.03	<0.03
80% scrap	0.39	0.27	0.06	0.22	2.44	<0.03	<0.03	<0.03	<0.03	<0.03	<0.03
100% scrap	0.43	0.28	0.07	0.23	2.37	<0.03	<0.03	<0.03	<0.03	<0.03	<0.03

From each of the batches, specimens in the shape of ingots and plates were cast (Figure 2) to characterize the alloy properties with the Profil Footprinter®, light microscope and micro-hardness.

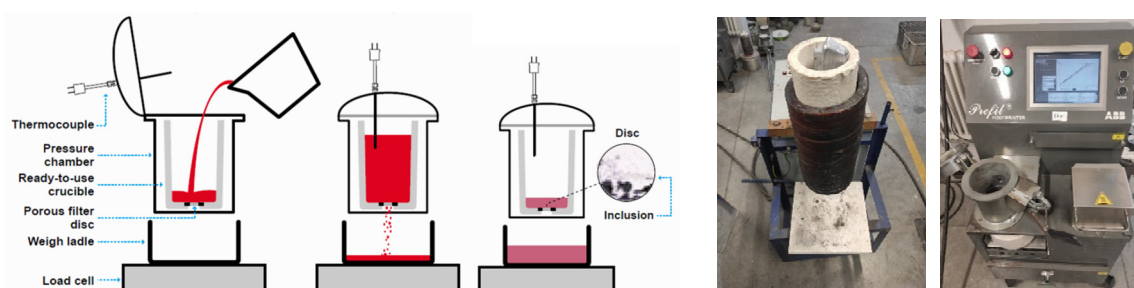


Figure 2. Images of the Profil Footprinter® equipment: scheme of the equipment [8] with the different parts and steps of the test (left), picture of the crucible (middle) and picture of the screen (right).

2.3. Filtration and Analysis by Means of Profil Footprinter®

Ingots produced for each of the material variants, with an average weight of 1.5 kg and approximate measures of 240 x 90 x 45 mm, were remelted for the Profil Footprinter® test, an instrument used to determine the amount and type of inclusions present in alloy, based on the pressure filtration principle. A ready-to-use crucible, equipped with a porous filter disc at the bottom, was pre-heated and installed in the pressure chamber. Then a sample of liquid metal, remelted at

730-740°C, was taken and poured into the crucible. The test started once the metal was at 700°C. During the test, the system continuously weighted the metal and displayed a curve of the accumulated weight versus the elapsed time.

Metallographic analysis consists of examining the residue of unfiltered metal collected on the filter surface of the Prefil Footprinter®. Because the Prefil Footprinter® device uses a filter with a pore size of 90 µm. The residue remaining in the filter were sectioned through the central plane perpendicular to the disc, ground and polished to a mirror-like finish. Metallographic examinations were observed on light microscopy (LM) Zeiss Axio Observer 7 and scanning electron microscope (SEM) Inspect F50 with Energy Dispersive X-ray Spectroscopy (EDS) EDAX chemical analysis in microareas. Research of the identification of inclusions involved the use of the EDS technique, which enables the analysis of the chemical composition in microareas on the sample surface. The quantitative analysis of inclusions was carried out on LM and SEM pictures. The content of the inclusions concentrated on the surface of the test filter is then quantified using image analysis software. This was then normalised by both nominal chord length, and by the mass of metal filtered, to give the familiar units of mm²/kg according to the generally accepted formula [18,19]. The inclusion concentration is reported in mm²/kg indicating area of inclusions in the sectioned part. There is no data available to confirm this statement, but it is considered to be valid by the industry. Inclusions are classified arbitrarily about the class and content (in mm²/kg).

2.4. Additional Tests

Tests were performed on the various material variants. The aim of these tests was to evaluate a property or characteristic relevant for each of the applications; this way, flowability was measured for HPDC alloys; hot compression behaviour for extrusion, and sheet metal samples were recrystallized and their hardness measured.

2.3.1. Flowability (HPDC Alloys)

A mould and procedure to assess aluminium alloy flowability were designed and tested [20] and a paper dedicated to flowability test results is currently under preparation. Flowability specimens, with 6 strips of different thicknesses (1, 3, 5, 7, 9 and 11 mm), were cast and measured to determine the alloy flowability of the batch produced with the different scrap level.

2.3.2. Hot Compression (Extrusion Alloys)

To evaluate the behaviour of the processability of the aluminium under extrusion conditions, hot compression tests were performed. Cylindrical samples 8 mm in diameter and 12 mm in length were extracted from the ingots and compressed in an Instron 5582 universal testing machine at a temperature of 500 ± 5 °C. Samples were heated for 15 minutes before testing, and the test was conducted as crosshead speeds of 250 and 450 mm/min until reaching 60% deformation. All contact points between the samples and the testing equipment were lubricated.

2.3.3. Production of Hot Deformed Samples (Sheet Metal)

In order to produce representative material for microstructure and hardness analysis, a hot deformation and recrystallization procedure was followed. The aim of this step was to transform the cast ingots into a microstructure comparable to a wrought alloy.

These samples were cut into small blocks, forged in a press to an approximate 40% reduction at 530 °C and finally annealed at 550 °C for 10 minutes and quenched, in order to force some recrystallization and break the casting structure.

After this, the samples were subject to post-processing: 6181A samples were then subject to artificial aging for 1 h at 200 °C. On the other hand, 5754 samples were cold formed at approximately 60% reduction to verify that the material showed the desired strain hardening behaviour; these conditions were chosen as relevant based on the work of Snopinski et al. [21].

3. Results

3.1. High Pressure Die Casting (HPDC) Alloys

3.1.1. Flowability Test Results

In order to assess processability of the EN AB-43500 alloy developed for HPDC a strip mould with different thicknesses was used. The length of the strips for the different samples investigated in the flowability test are presented in Table 7.

Table 7. Length measured for the 6 strips of the flowability specimen and average value.

	1 mm	3 mm	5 mm	7 mm	9 mm	11 mm	Average
Ref. ingot	0	135	35	135	60	85	75.00
20% scrap	0	100	55	110	95	70	71.67
40% scrap	0	90	40	80	65	60	55.83
60% scrap	0	130	30	105	75	20	60.00
80% scrap	0	40	5	70	20	0	22.50
100% scrap	0	70	5	75	20	10	30.00

It can be observed that, in general, the materials obtained with a higher amount of scrap show lower flowability than the ingot or those with lower scrap content. Another observation that can be made is that, in general, the metal flows better in the right side of the mould (channels 3, 7 and 9 mm thick) than in the left side of the mould (1, 5 and 11).

3.1.2. Microstructure

The observation of polished specimens extracted from the produced square plates (Figure 1) revealed a similar microstructure for all 6 scrap proportions. No new phases or foreign particles were detected in the specimens with a higher scrap content, neither a significative difference in shape or size of the different phases was observed (Figure 3).

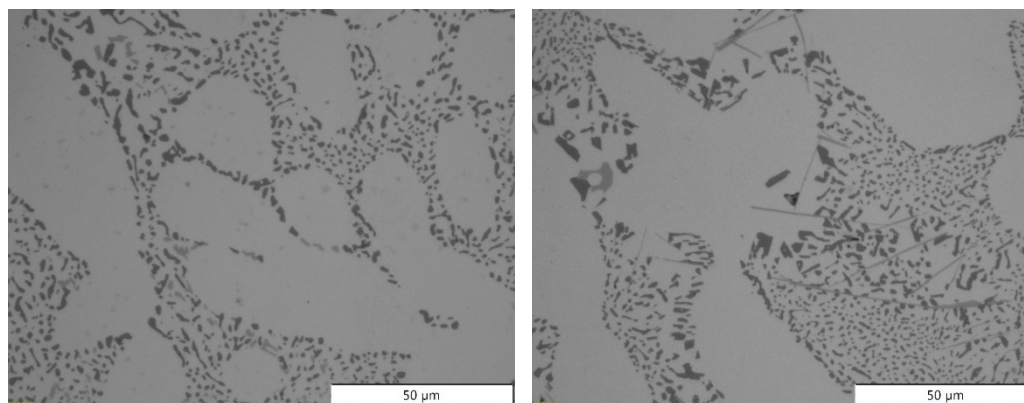


Figure 3. Microstructures obtained by light microscope for the most extreme batches produced for EN AB-43500 alloy: 0% scrap (left), and 100% scrap (right).

3.1.3. Prefil Footprinter®

Table 8 summarises the main results of the Prefil Footprinter® test. For each of the alloys, a decrease in the rate of filtration is observed with an increase in the proportion of scrap used. The filtration rates obtained for the 43500 alloy decreased when the proportion of scrap in the alloy was increased. It was observed that samples with 0 and 20 % scrap content presented a high filtration rate of 17-14 g/s, 40 %-60 % the filtration rate was decreased to about 13 g/s and samples with 80 and 100% scraps was about 10 g/s.

Table 8. Values obtained from the Prefil Footprinter® test of the EN AB-43500 alloy.

Samples	0% scrap	20% scrap	40% scrap	60% scrap	80% scrap	100% scrap
Weight (kg)	1.416	1.432	1.406	1.415	1.403	1.402
Duration (s)	85	100	109	112	134	140
Filtration rate (g/s)	16.7	14.3	12.9	12.6	10.5	10.0

It is observed that an increase in the amount of scrap led to a higher filtration time caused by an increase in the amount of settled contaminants in the filter.

Samples from the filtered inclusions were cut and a metallographic analysis was performed on the polished surfaces close to the ceramic filter where the inclusions were located. The samples were analysed using SEM. Figure 4B–I shows the EDS elemental mapping analysis for the SEM image (Figure 5a) of while the results of quantification of the microinclusions are shown in Figure 5.

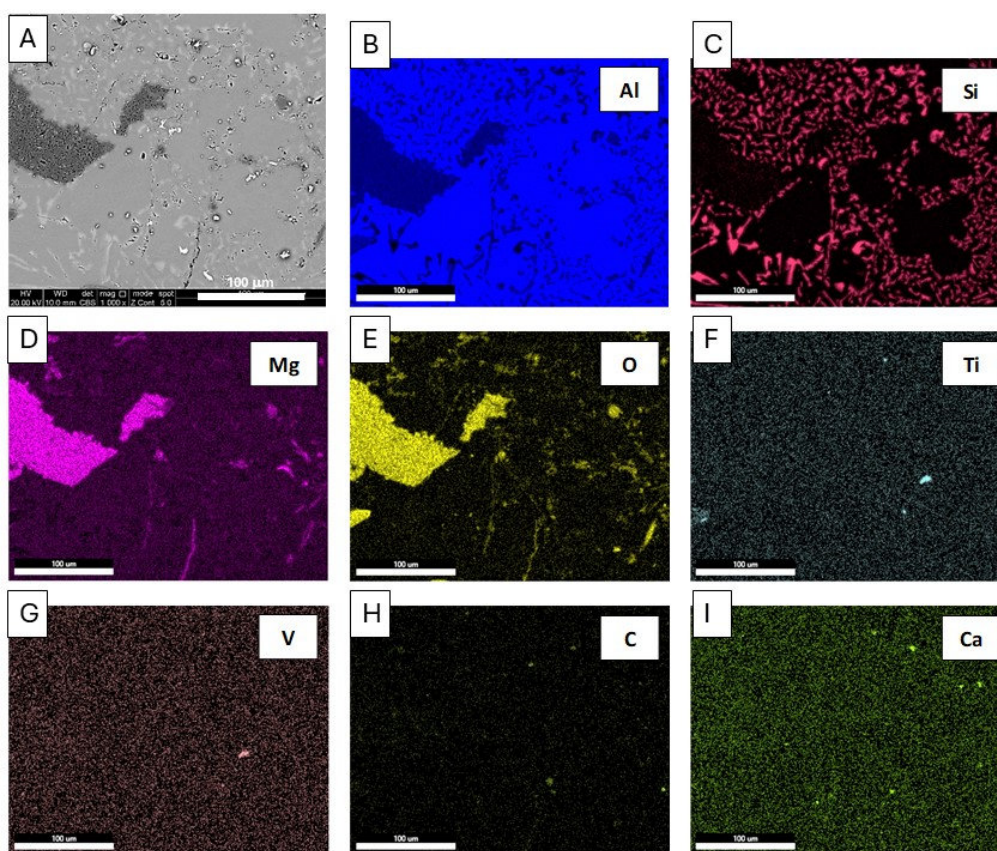


Figure 4. Microstructure (a) and energy-dispersive X-ray spectroscopy (EDS) maps (b-i) of distribution of elements: Al, Si, Mg, O, Ti, V, C, Ca, SEM of the EN AB-43500 alloy.

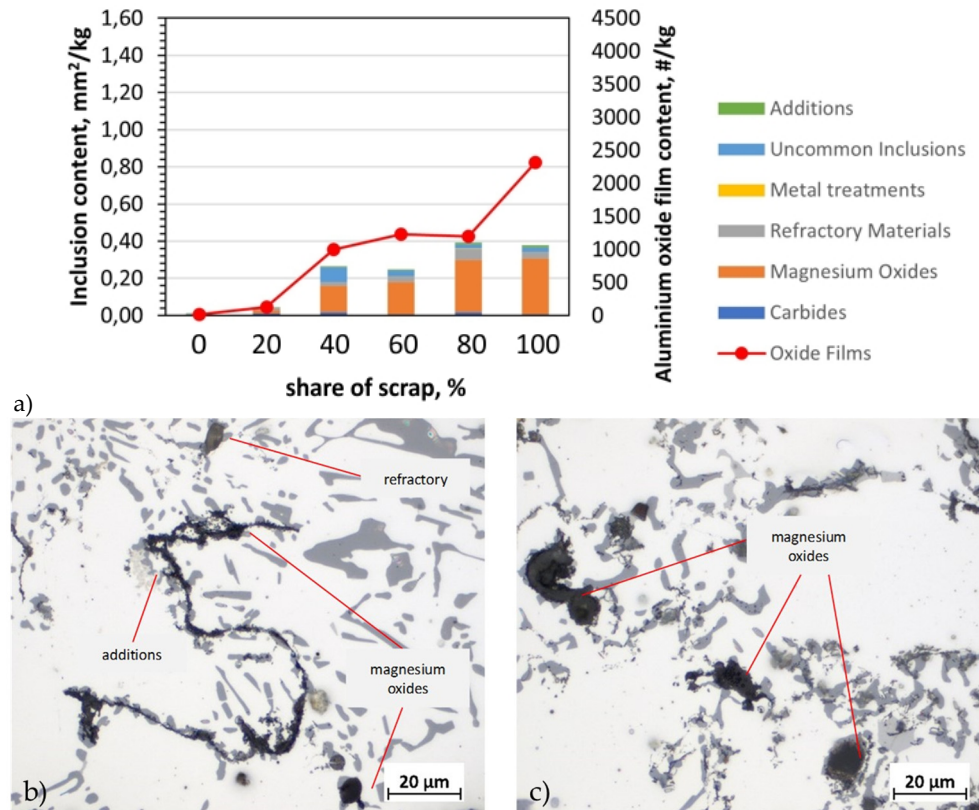


Figure 5. Analysis of inclusions in AB-43500 alloy variants: a) summary of identified inclusions and quantification of oxides; b) microstructure with identified types of inclusions in a sample containing 20% scrap; c) microstructure with identified types of inclusions in a sample containing 80% scrap; LM.

The elemental distribution profile obtained by the mapping (Figure 5) technique shows that the dark inclusion compounds are rich in Mg, O and/or Al which were identified as magnesium oxides and spinel, the brighter compounds are rich in Ti and V which were identified as additions. In addition, was observed the presence of compounds rich in Si or Ca and O, which were identified as refractory materials, and also revealed carbides were compounds are rich mainly in C.

Analysis of chemical composition of inclusions above the filter in the tested samples of alloy 43500 (Figure 5) shows that the highest part of the fraction was magnesium oxides (MgO, MgAl₂O₄ - cuboid, MgAl₂O₄ - spinel). For pure alloy with 0.2% Mg, the total inclusion content (TIC) was 0.01 mm²/kg while sample containing 80% and 100% scrap, TIC was approx. 0.4 mm²/kg.

3.2. Extrusion Alloys

3.2.1. Microstructure

The microstructure of the extrusion alloys was similar, regardless of the amount of scrap used, showing a typical solidification structure composed of alpha grains surrounded by low melting point constituents, segregated to the grain boundaries. The microstructures observed on LM corresponding to the 100% scrap ingot are presented in Figure 6.

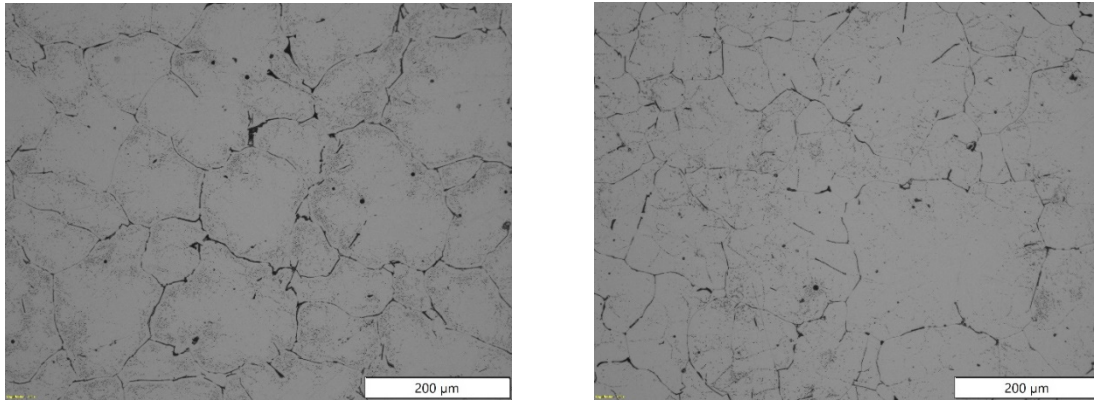


Figure 6. Microstructures obtained by light microscope for the most extreme batches produced for 6063 alloy: 0% scrap (left), and 100% scrap (right).

Notably, this cursory OM investigation did not detect a significantly different amount of inclusions. To better refine this assessment, samples were subject to the filtration and analysis procedure previously used for HPDC alloys. Results are described in the following section.

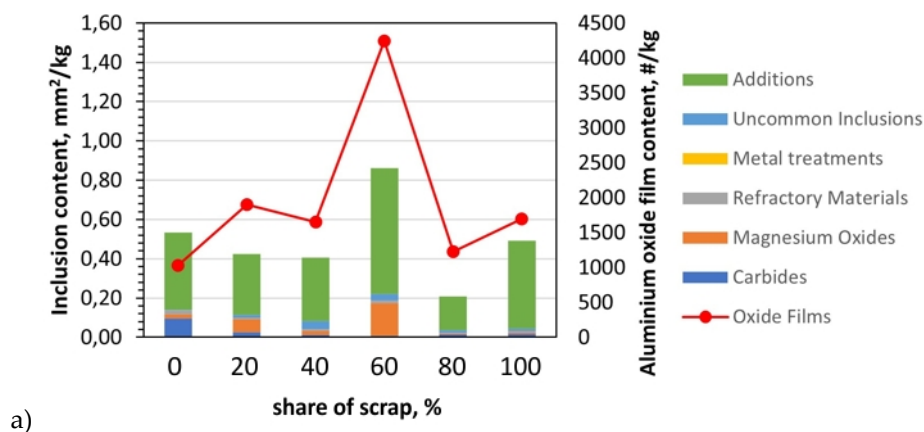
3.2.2. Analysis of Inclusions by Means of Prefil Footprinter

The presence of inclusions was analysed in detail using the Prefil Footprinter[®] in a manner analogous to the study presented for HPDC alloy. Table 9 shows the results of the experiment carried out. The amount of scrap did not significantly affect the filtering speed for the 6063 extrusion alloy. In the case of alloy 6063, for samples with a scrap content 0 to 100%, the filtration rate was low and at a comparable level, which was about 5 g/s.

Table 9. Values obtained from the Prefil Footprinter[®] test of the 6063 extrusion alloy.

Samples	0% scrap	20% scrap	40% scrap	60% scrap	80% scrap	100% scrap
Weight (kg)	0.687	0.632	0.77	0.649	0.747	0.749
Duration (s)	150	150	150	150	150	150
Filtration rate (g/s)	4.6	4.2	5.1	4.3	5.0	5.0

The samples were analysed using SEM. Figure 8B–I shows the EDS elemental mapping analysis for the SEM image of Figure 8 A while the results of quantification of the microinclusions are shown in Figure 7.



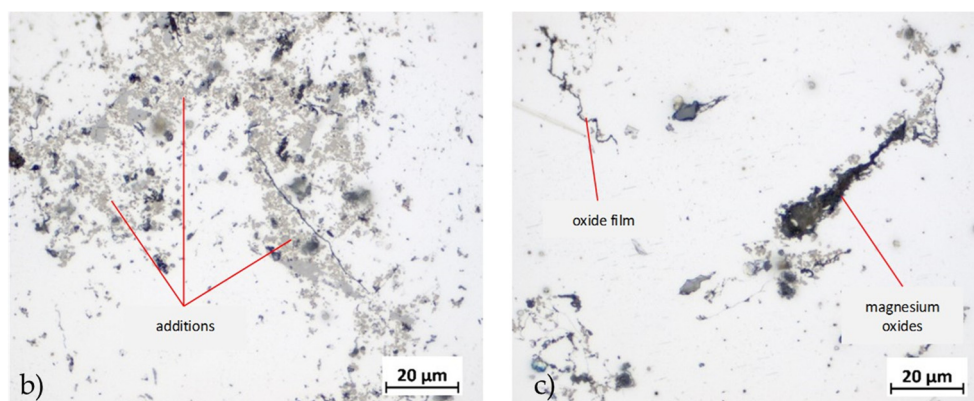


Figure 7. Analysis of inclusions in 6063 extrusion alloy variants: a) summary of identified inclusions and quantification of oxides; b) microstructure with identified types of inclusions in a sample containing 20% scrap; c) microstructure with identified types of inclusions in a sample containing 80% scrap; LM.

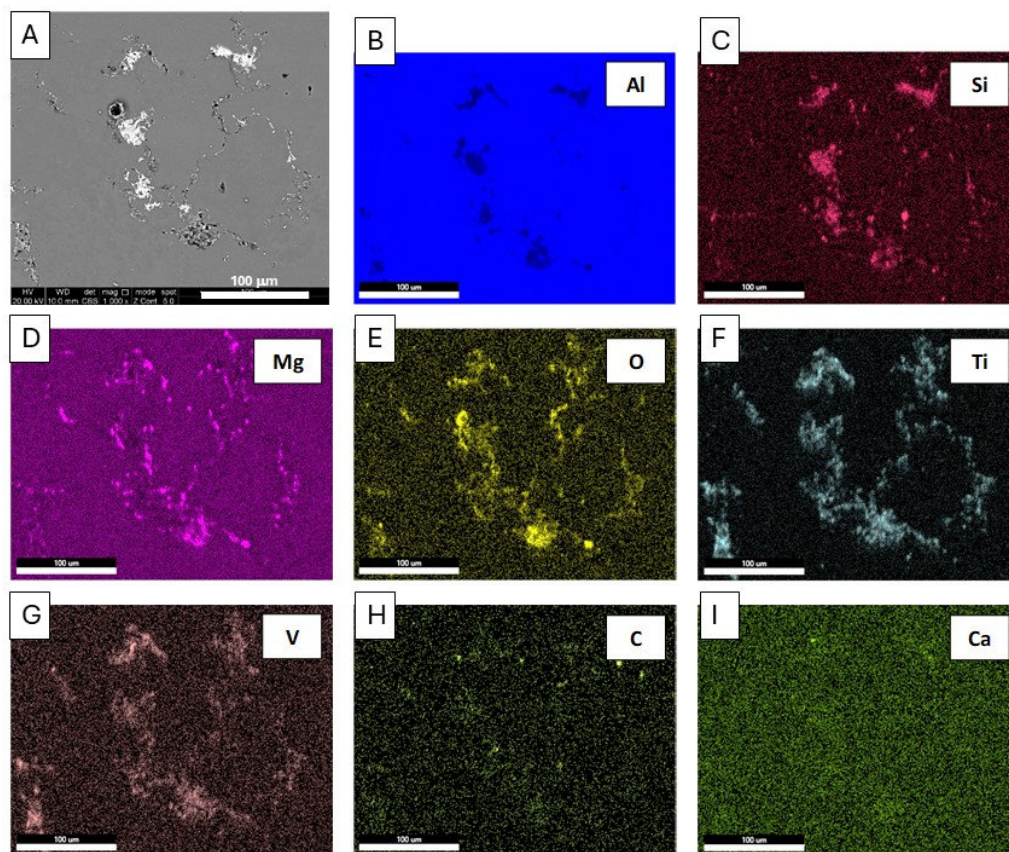


Figure 8. Microstructure (a) and energy-dispersive X-ray spectroscopy (EDS) maps (b-i) of distribution of elements: Al, Si, Mg, O, Ti, V, C, Ca, SEM of the 6063 extrusion alloy.

The elemental distributions produced by the mapping technique for alloy 6063 show areas rich in Mg, O, Ti and V (Figure 8). In addition, C-enriched areas were revealed, which were identified as carbides.

The results of the metallographic analysis, shown in Figure 7, revealed that the 0 to 100% scrap samples showed a higher proportion of additives (0.2-0.6 mm²/kg) than magnesium oxides (0.006-0.17 mm²/kg). A non-major scatter of TIC in the range of 0.4 - 0.5 mm²/kg was determined for the samples except for the 60 and 80 % scrap. The sample containing 60% scrap was the most contaminated (TIC over 0.8 mm²/kg). In addition to additives, a significant proportion of magnesium

oxides were found in the alloy structure of this sample. The lowest TIC of 0.2 mm²/kg and trace amounts of magnesium oxides were found in the sample with 80 % scrap content.

3.2.3. Compression Tests

Compression tests were carried out at two crosshead speeds of 250 mm/min and 450 mm/min, simulating the metal flow rate during extrusion. Samples were deformed up to 60 %. The results obtained from the compression tests are presented in Figure 9 (250 mm/s) and Figure 10 (450 mm/s).

The curves in the actual stress-strain diagrams clearly show that at a crosshead speed of 250 mm/min, none of the samples with different scrap contents deviated significantly from the average during the extrusion process. Compression tests carried out at 450 mm/min showed differences in stress levels compared to compression tests at 250 mm/min on samples with different scrap contents. Compression tests at a higher speed (450 mm/min) showed a higher yield strength of approximately 3 MPa compared to samples deformed at a lower speed (250 mm/min).

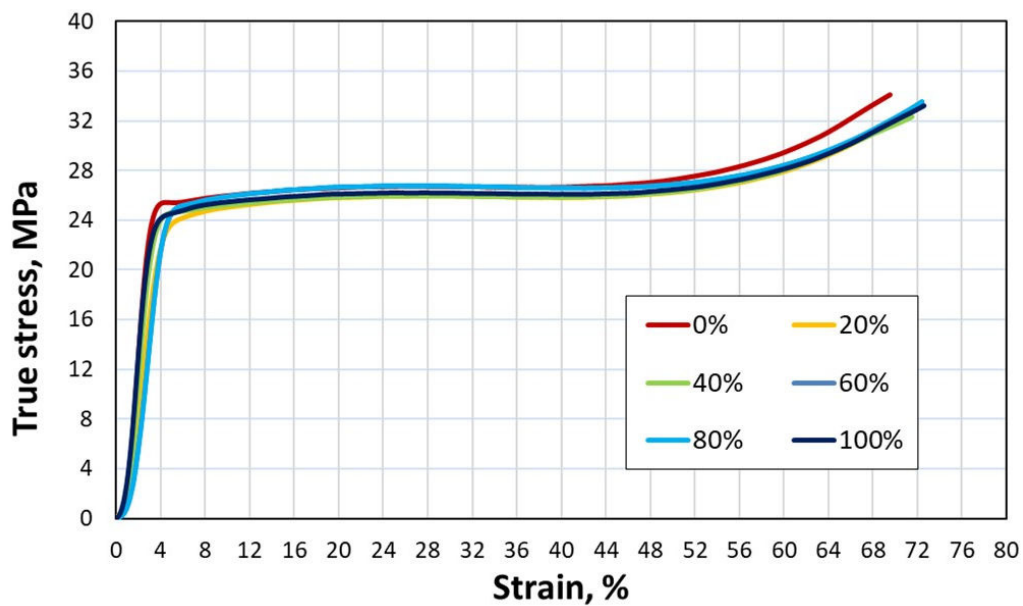


Figure 9. True stress-strain curves from compression tests crosshead speed 250 mm/min.

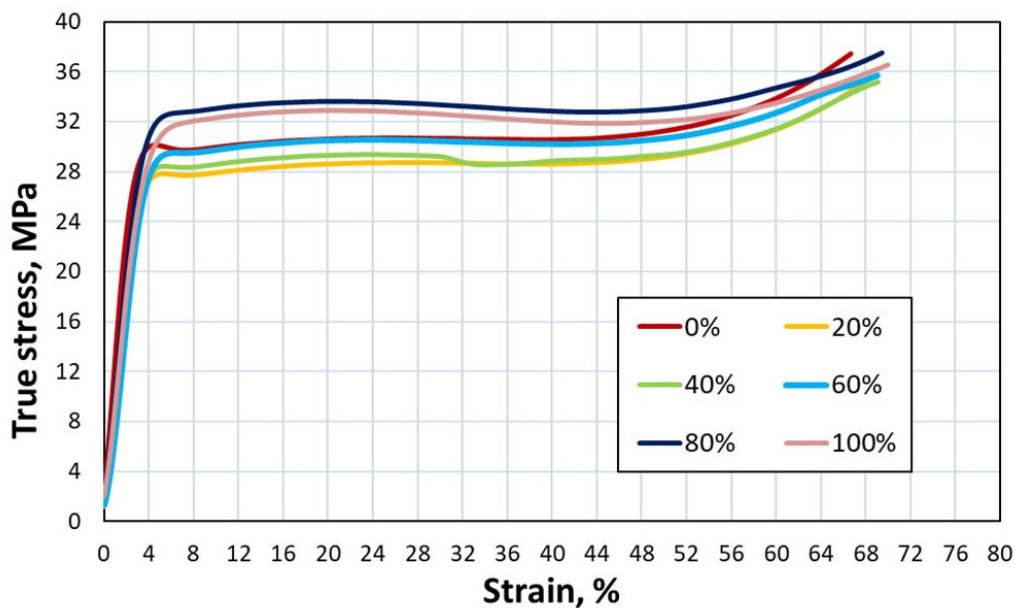


Figure 10. True stress-strain curves from compression tests crosshead speed 450 mm/min.

3.3. Sheet Metal Alloys

3.3.1. Microstructure

Basic microstructural analysis was performed in order to determine if the different amount of recycled material affected microstructure in a relevant way. A basic plastic deformation and recrystallization procedure was followed (Section 2.4.3) to ensure that the casting microstructure was transformed into a hot formed microstructure more representative of a wrought product.

As-cast ingots (left column in Figure 11 for 6181A, Figure 12 for 5754) show a reticular structure, composed by low-melting point phases surrounding alpha grains, suggesting a dendritic microstructure with non-alpha phases segregated in the grain boundaries in eutectic-like formations. This structure and phase composition is repeated for all scrap amounts and in both 5754 and 6181. It is worth to comment that the amount of scrap does not seem to have an impact on the structure or presence of macro phases.

Deformed samples (right column in Figure 11 for 6181A, Figure 12 for 5754) show how plastic forming and recovery mechanisms have broken the as-cast structure. Clearly elongated grains can be recognized, particularly for the cold formed 5754 alloy. However, the overall microstructure still presents a high degree of segregation, with silicon-based particles concentrating in the alpha-grain boundaries. In this regard, the proposed experiment generates a structure closer to that of a wrought product, but not entirely equivalent to a rolled sheet.

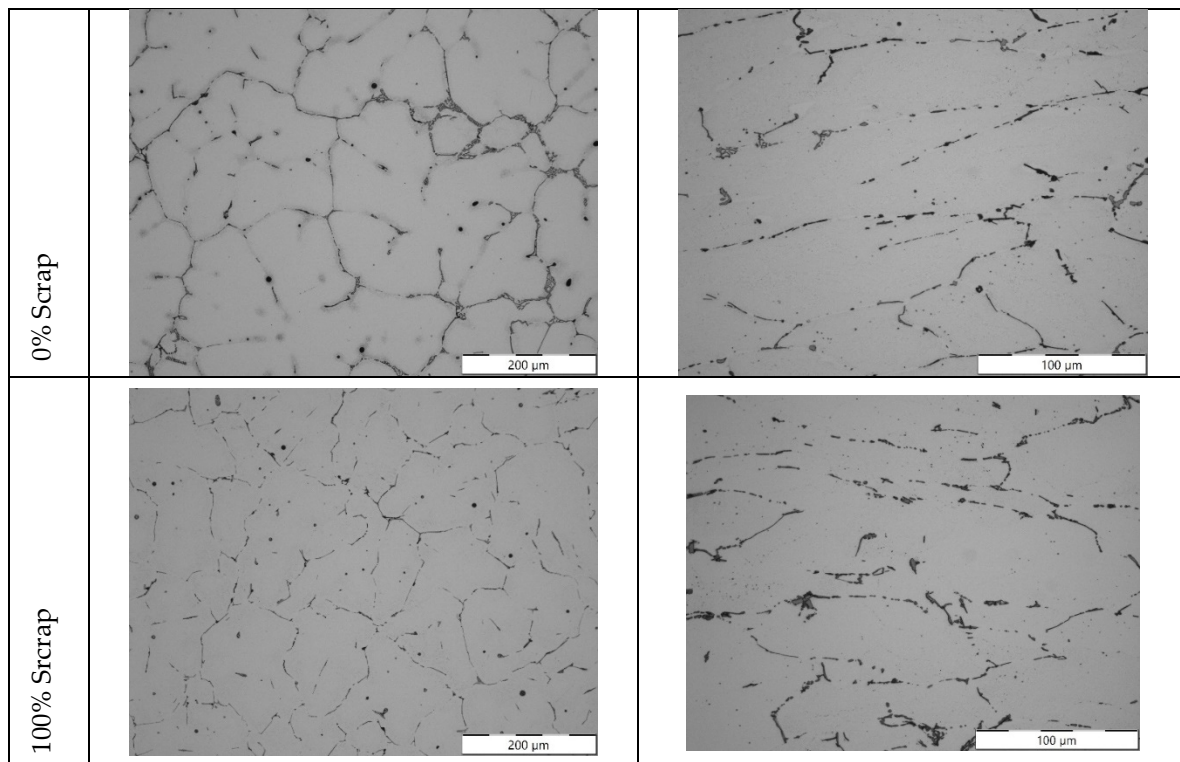


Figure 11. Microstructures for the different batches produced for 6181A alloy: extreme cases of 0 and 100% scrap as cast (left column) and after processing by 40 % hot deformation and 65 % cold reduction (left column).

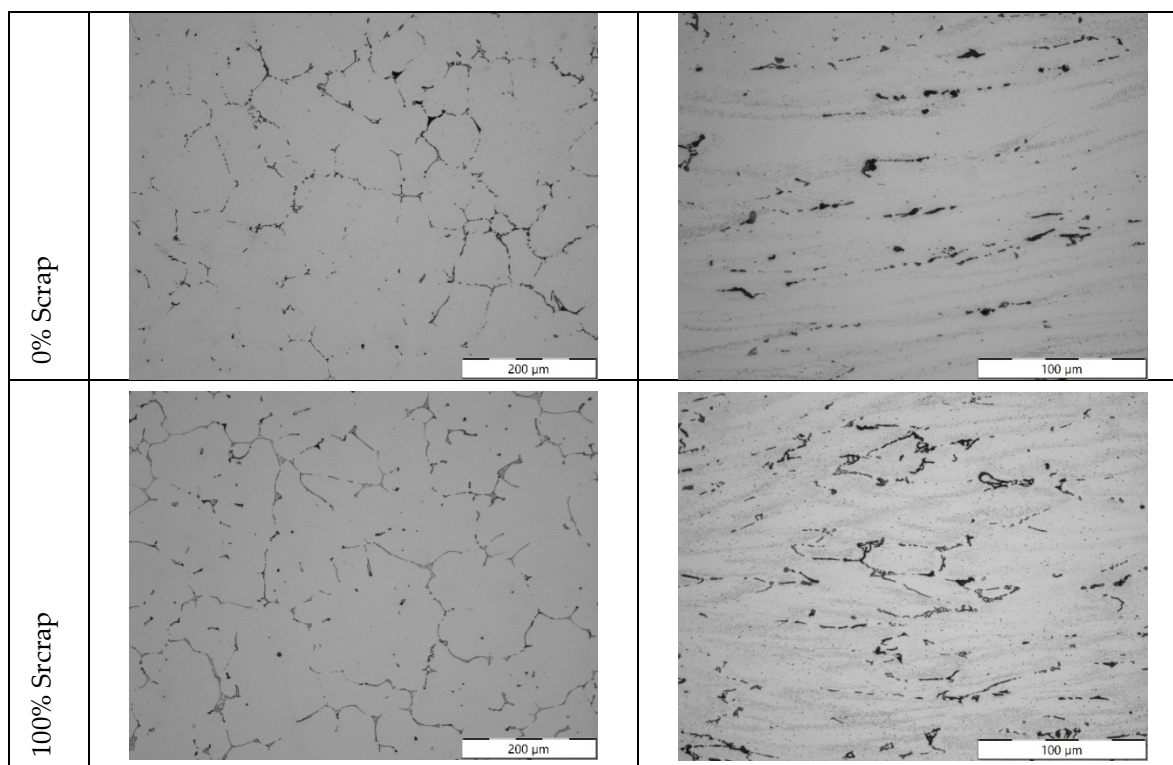


Figure 12. Microstructures for 5754 alloy: extreme cases of 0 and 100 % scrap as cast (left column) and after processing by 40 % hot deformation and 65 % cold reduction (left column).

In the Light Microscopy analysis of these samples, the presence of inclusions does not appear to significantly differ for the varying percentages of scrap. While some oxides or Fe-based phases can be occasionally found, these do not appear to follow particular relationship with the amount of scrap used in casting.

3.3.2. Analysis of Inclusions by Means of Prefil Footprinter

As done for the previous cases, detailed characterization of inclusions would be performed through the specific filtration and analysis method described in the experimental section.

For alloy 6181, the analysis of the filtration rate (Table 10) did not show a clear influence of the amount of recycled material in the range of 0-80 % (7.5-8.8 g/s), whereas for the sample with the highest amount of scrap (100 %) the filtration becomes slower (6.2 g/s). However, this result does not seem to be related to the presence of inclusions in the material.

Table 10. Values obtained from the Prefil Footprinter® test in 6181A variants.

Samples	0% scrap	20% scrap	40% scrap	60% scrap	80% s crap	100% scrap
Weight (kg)	1.127	1.287	1.323	1.247	1.273	0.934
Duration (s)	150	150	150	150	150	150
Filtration rate (g/s)	7.5	8.6	8.8	8.3	8.5	6.2

The samples were analysed using SEM. Figure 13B–I shows the EDS elemental mapping analysis for the SEM image of Figure 13A while the results of quantification of the microinclusions are shown in Figure 14.

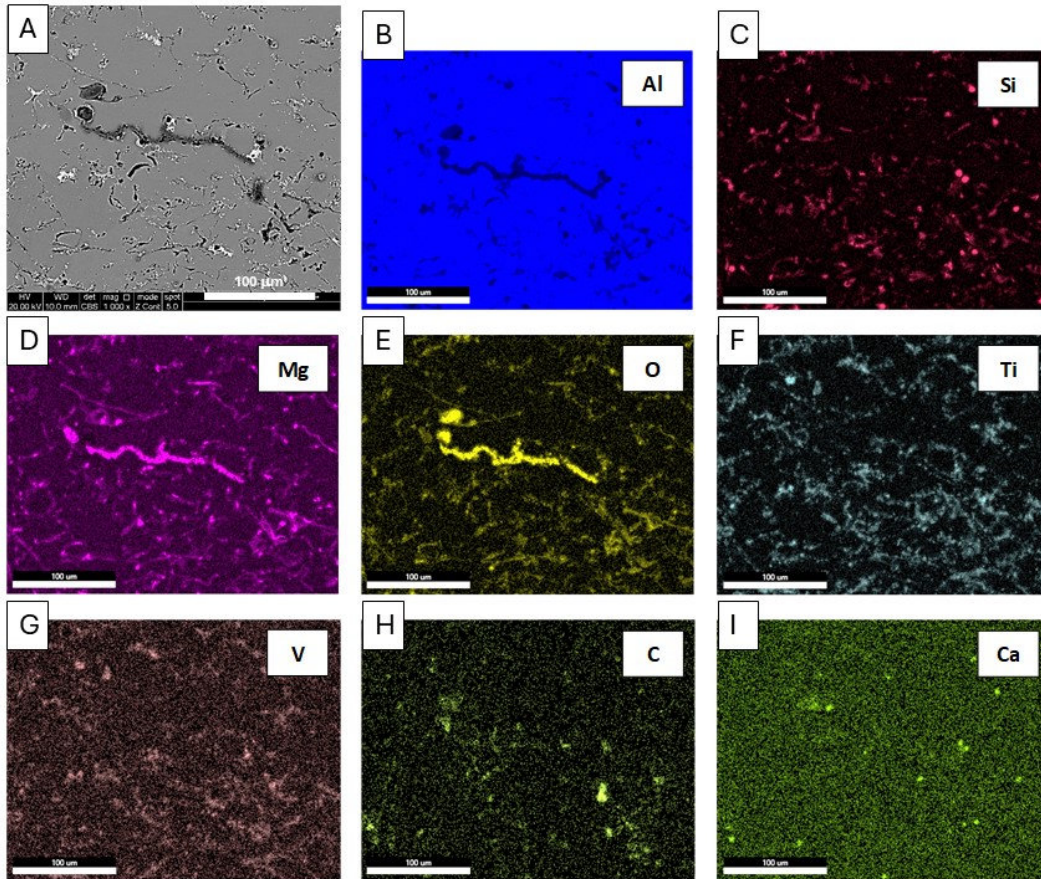


Figure 13. Microstructure (a) and energy-dispersive X-ray spectroscopy (EDS) maps (b-i) of distribution of elements: Al, Si, Mg, O, Ti, V, C, Ca, SEM of the 6181 alloy.

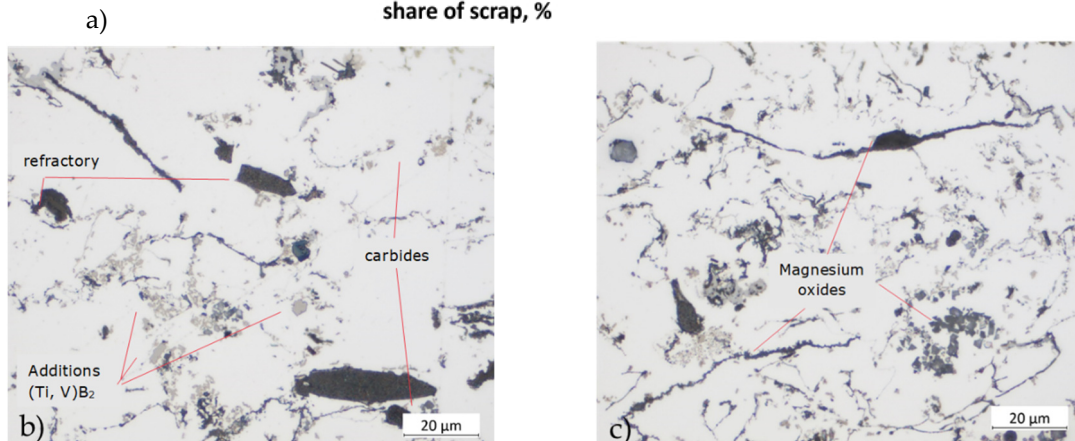
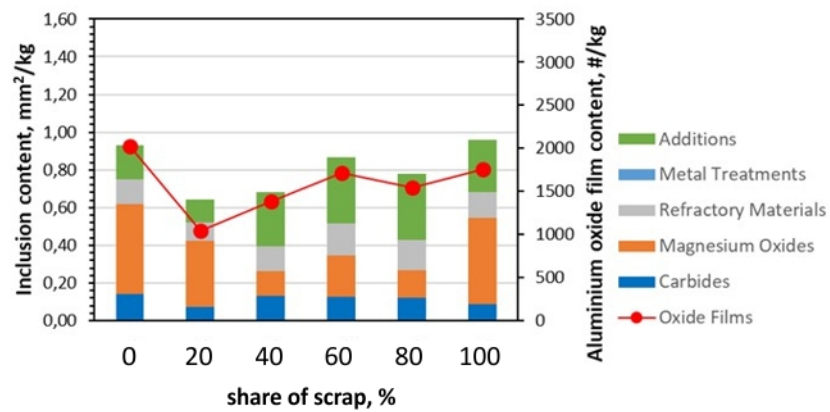


Figure 14. Analysis of inclusions in 6181A variants: a) Summary of identified inclusions and quantification of oxides; b) identification of refractory inclusions, carbides and additions on a 40% scrap sample; c) magnesium oxides (thin and layer-like) in 80% scrap sample.

Analyses of the elemental distribution maps of alloy 6181 show the presence of impurities similar to those found in alloy 6063 for extrusion. Regions rich in Mg, O and Ti, V were found and numerous regions containing Ca, Si and C with Ca or Al compounds.

The highest levels of impurities were found in both the pure alloy and the 100 % alloy. High levels of magnesium oxide, additions, refractories, carbides and oxide films were found in the samples tested. The presence of magnesium oxides determined the high level of impurities in the pure 6181 alloy.

In the case of alloy 5754, the analysis of the filtration rate (Table 11), derived from a show no clear influence of the recycling amount, with all filtration rate values being very similar around 8 g/s.

Table 11. Values obtained from the Prefil Footprinter® test in 5754 variants.

Samples	0% scrap	20% scrap	40% scrap	60% scrap	80% scrap	100% scrap
Weight (kg)	1.115	1.272	1.236	1.217	1.232	1.278
Duration (s)	150	150	150	150	150	150
Filtration rate (g/s)	7.4	8.5	8.2	8.1	8.2	8.5

The samples were analysed using SEM. Figure 15B–I shows the EDS elemental mapping analysis for the SEM image of Figure 15A while the results of quantification of the microinclusions are shown in Figure 16.

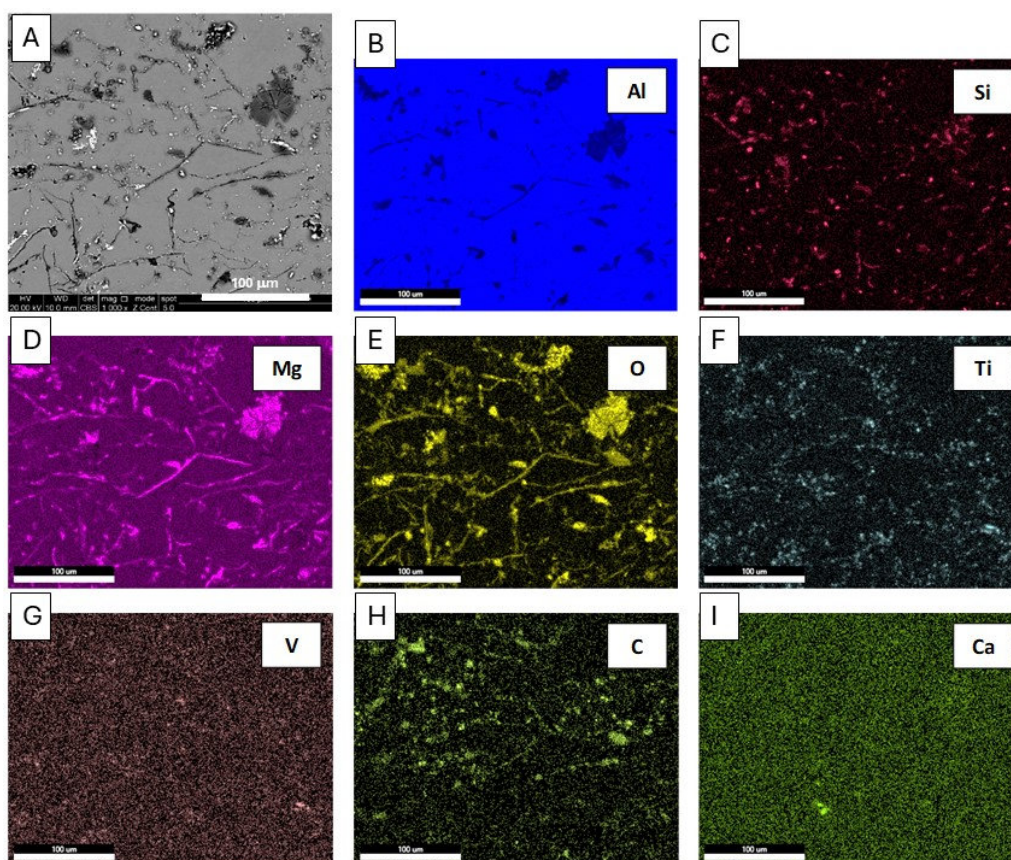


Figure 15. Microstructure (a) and energy-dispersive X-ray spectroscopy (EDS) maps (b-i) of distribution of elements: Al, Si, Mg, O, Ti, V, C, Ca, SEM of the 5754 alloy.

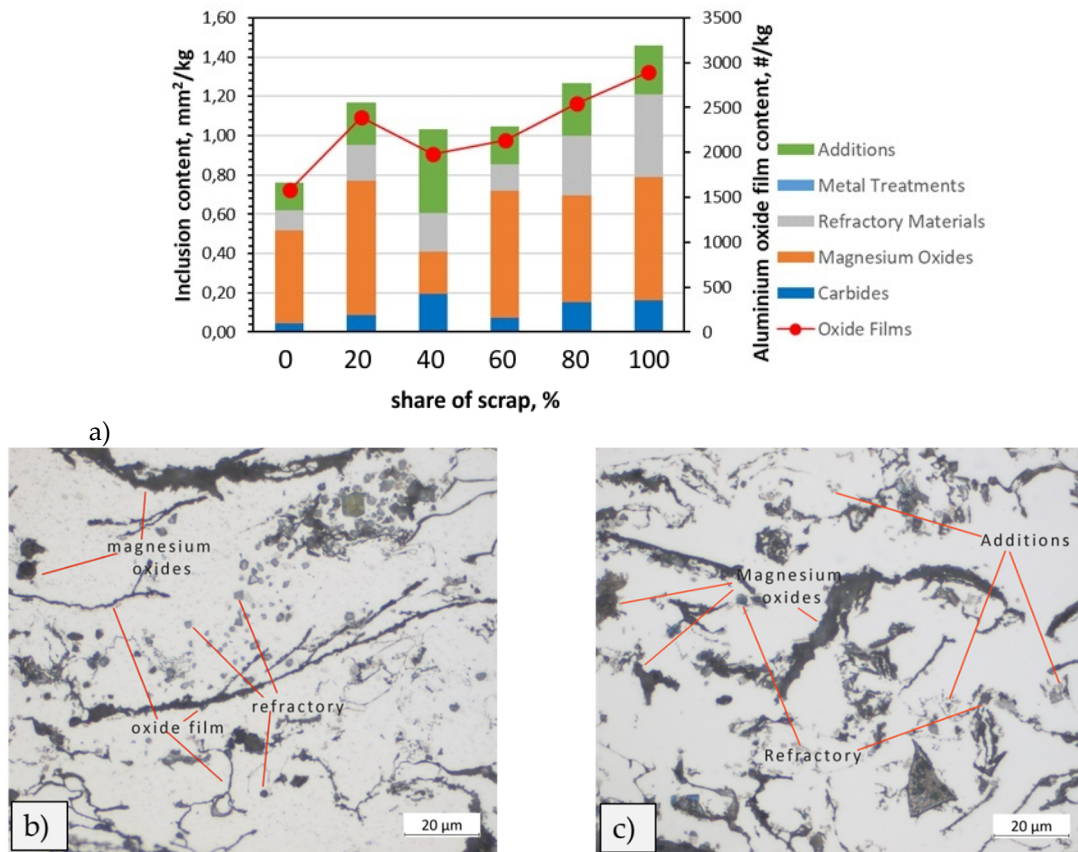


Figure 16. Analysis of inclusions in 5754 variants: a) Summary of identified inclusions and quantification of oxides; b) identification of refractory inclusions, carbides and additions on a 40% scrap sample; c) high presence of magnesium oxides and oxide films in 100% scrap sample.

Detailed analysis shows a very high inclusion content for this material, which increases with recycling steps, together with the presence of oxide films.

The chemical composition of the inclusions above the filter in the samples of alloy 5457 tested shows that the largest part of the fraction was magnesium oxides, which is related to the high magnesium content in the alloy (about 3 % by weight). For the pure alloy, the TIC was 0.761 mm²/kg. For a sample containing 100% scrap, the TIC was approximately 1.5 mm²/kg, which was the highest amount of samples analysed. In the alloy analysed, an increasing amount of refractory material was found as the scrap content increased. Additives were observed at similar levels in all samples of 5754 alloy analysed.

3.3.3. Mechanical Properties

In terms of mechanical properties, in both cases the effect of recycling is not apparent. For 6181A alloys (Table 12), virtually the same hardness level is attained in the three studied conditions.

Table 12. Hardness values measured on 6181A-based samples.

Scrap level	Hot Formed		Aged	
	% Reduction	HV1	Treatment	HV1
0%	42%	66 ± 2	1h 200 °C	86 ± 3
40%	35%	67 ± 3	1h 200 °C	84 ± 3
100%	44%	67 ± 3	1h 200 °C	82 ± 3

For 5754 (Table 13), initial hardness differs between the three hot formed samples; however, this believed to be related to the different degree of effective reduction attained in each case. However, for samples annealed and cold formed, an equivalent hardness is reached (95 HV) regardless of

recycling amount. This is a noteworthy result, as the chemical composition in this case differed notably in terms of Silicon and Magnesium: 0.1% Si and 2.8% Mg for 0% scrap samples, and 0.4% Si and 2.4% Mg for 100% scrap. However, in all cases a level of hardness is obtained compatible with work-hardened 5754.

Table 13. Hardness values measured on 5754-based samples.

Scrap level	Hot Formed		Cold Worked	
	% Reduction	HV1	% Reduction	HV1
0%	35%	71 ± 3	66%	94 ± 3
40%	35%	71 ± 3	67%	94 ± 3
100%	42%	85 ± 3	64%	95 ± 3

4. Discussion

In this study, the following series of alloys were tested in the processes: AB-43500 alloy for HPDC, 6063 for extrusion and 6181A, 5754 for stamping with different scrap. The effects of compression test at elevated and reduced temperatures on microstructure and properties were also investigated.

The effect of increasing scrap content on the properties of the alloys studied was comparable. An increase in various types of impurities with increasing scrap content was found in all alloy grades tested. Large differences between the AB-43500 casting alloy and the alloys for plastics processing were found in the rates of liquid metal flow through the Prefil Footprinter® filter (Figures 5 and 10). This appears to be related to the flowability of the alloys. Casting alloys, especially for HPDC casting, are characterised by very good flowability [21,22], which is also confirmed by the tests carried out in this study (Table 8). It can also be concluded that an increasing amount of scrap leads to a decrease in flowability. However, the general microstructural analysis of the specimens did not reveal the presence of new phases or big foreign particles that could be observed in the light microscope, neither for HPDC (Figure 3) or the other processing routes investigated in the present work (Figures 6, 11 and 12), even if these differences were detected in the more detailed Prefil Footprinter® analysis, particularly in the case of HPDC. This suggests that the main difference is in the presence of small non-metallic particles, such as oxides, present in the scrap or generated by the oxidation produced during the melting process due to the presence of residues in the scrap. Even though this small contamination does not translate into microstructural changes, it does highly affect alloy flowability.

Typical oxides in film and cuboid particle form were identified with different compositions. Metallographic examination of the filter for the AB-43500 alloy showed that the magnesium oxides content and refractory materials, which include Al₂O₃ and CaO, increased with the amount of scrap. According to studies [6,12,22], these are typical impurities for this type of alloy due to the Mg content. The magnesium content increased with the addition of scrap. In the pure AB-43500 alloy it was 0.18 wt.%, while in the same alloy cast from 100% scrap it was 0.25 wt.%. Regarding to oxides from the refractory, they can enter the melt through abrasion of the furnace and channel lining, and are usually silicates or other complex oxides, which may also contain Na, K and Ca [7,15]. In addition to the prevalent oxides, (Ti,V)B₂ inclusions also were observed. Especially in the case of alloys 6063 and 6181A, which are intended for extrusion and plastic stamping, despite the higher Mg content in the structure, additives, i.e., (Ti, V)B₂ agglomerations were present above the filter in a significant quantity. Their presence is confirmed by studies carried out by other researchers [9]. In both our own research (Figure 10) and that of others [23,24], borides have been found to inhibit the flow of liquid metal through the Prefil Footprinter® filter. According to the authors of Yang et al. [25] the reduction of efficiency is due to the strong adherence of TiB₂ particles to oxide films in the filter. The adherence and agglomeration of heavy grain refiner particles onto light oxide films counter the gravitation number of oxide films, making them difficult to be filtrated [25]. This can also lead to inhibition of the filtration process during alloy casting. TiB₂ inclusions are hard and have adverse effects on extrusion and machining tools [6].

This can be confirmed by a slight increase in strength as the scrap content of the 6063 alloy increases during the compression test (Figures 9 and 10). According to literature [26] TiB₂ particles could tend to agglomerate which could lead to the formation of thick oxides. This is related to the presence of a superficial aluminide layer in Al-Ti-B. Therefore, it is necessary to check the chemical composition with regard to Ti and B content before the casting process to overcome particle agglomeration problems. In addition, 6181A alloy contained MgO due to its even higher Mg content.

In the 5754 and 6181A alloys, high levels of impurities such as magnesium and aluminium oxides and additives were found after the addition of 100% scrap. This is particularly true for 5754. In Al-Mg alloys, the tendency to oxidize increases rapidly with increasing Mg content [13,14]. The results obtained during the analysis (Figure 15) are consistent considering the high magnesium content of this alloy, as can be observed in the chemical analysis of the ingots presented in Table 8, where the Mg level decreased with each recycling step. It is likely that some of the added Mg, as well as the alloying elements already present in the melt, were lost to the slag during melting experiments.

In addition, presence of carbides was revealed (Figures 15 and 16). According to literature [7] melting scraps with organic contaminations can lead to an increased amount of carbide formation. During the smelting process, organic impurities can react with aluminium and other elements. These reactions can lead to the formation of carbides in the alloy. The recycling-friendly coating removal practices proposed by the authors [27] which involve thermal treatment (pyrolysis) of scrap before it is smelted, may avoid this problem.

Studies relating to the thermo-mechanical treatment of alloys for the stamping process did not reveal any effect of scrap content on properties, despite the variations in chemical composition. Alloy 5754 showed strengthening due to cold work, reaching about 95 HV1 hardness for the three compared compositions despite decreasing Mg content. Similarly, 6181A showed similar level of age hardening after a treatment cycle. The study shows that an alloy produced with 100% scrap content will not adversely affect the mechanical properties, as long as chemical composition is kept within reasonable ranges.

This observation is consistent with the results of reference [12]: in that work, increased recycling content of alloy 6181 did not result in modification of monotonic mechanical properties, even though it did result in a loss of formability in terms of FLD curve.

5. Conclusions

It is possible to obtain high quality aluminium alloys within the range defined in the standards with a high proportion of selected scrap, close to 100%, and the addition of the required elements. The overall microstructural analysis did not reveal the presence of new phases or large foreign particles in the samples, indicating the stability of the microstructure in the alloys tested.

- Using careful scrap selection, it was possible to produce high quality recycled aluminium alloys. However, unwanted elements were introduced in the cases where scrap selection was not excellent. This reinforces scrap selection as a major area of research in circular economy related to structural metals.
- For alloys with high Mg content, oxidation of Magnesium caused reduced content in the final composition of the samples, as well as presence of oxide inclusions. Therefore, even in recycling-intensive material production, some Magnesium will need to be added in addition to reclaiming the element contained in the sourced scrap.
- Detailed Prefil Footprinter® analysis revealed significant differences in the content and nature of inclusions in aluminium alloys, mainly oxides, additives and carbides, which are important for HDCP, extrusion and stamping processes.
- Although the observed differences in non-metallic particle content do not affect microstructural changes, they do have a significant effect on melt flowability, which is critical for HDCP processes. For EN AB-43500 alloys intended for casting, an increase in the scrap content results in an increase in the magnesium oxide content, which reduces the castability of the alloy.
- 6063 alloys intended for extrusion were characterised by a high level of additives, the proportion of which was independent of the amount of scrap used.

- Sheet metal alloys 6181A and 5754 showed no modification in monotonic mechanical properties due to recycling. However, differences were observed in terms of inclusions. Alloy 6181A, similar to 6063, shows no change in impurity content with increasing scrap content, whereas in alloys 5754 an increase in scrap content results in an increase in the amount of magnesium oxides.

Author Contributions: Conceptualization, M.dS. (Manel da Silva) and J.P. (Jaume Pujante); methodology, M.dS, J.P., J.H.-W. (Joanna Hrabia-Wiśnios), B.A. (Bogusław Augustyn), D.K. (Dawid Kapinos), M.W. (Mateusz Węgrzyn); validation, M.dS, J.P., J.H.-W., S.B. (Sonia Boczkal); formal analysis, M.dS, J.P., S.B., J.H.-W.; investigation, M.dS, J.P., J.H.-W.; B.A., D.K., M.W. resources, M.dS., J.H.-W., S.B.; data curation, M.dS, J.P., J.H.-W, S.B.; writing—original draft preparation, M.dS., J.P.; writing—review and editing, M.dS., J.P., S.B., J.H.-W., B.A., D.K.; visualization, M.dS., J.P., S.B., J.H.-W.; supervision, M.dS.; project administration, M.DS.; funding acquisition, M.DS. All authors have read and agreed to the published version of the manuscript.

Funding: The research was carried out as part of SALEMA project that received funding from the EU research and innovation program Horizon 2020 under grant agreement No. 101003785.

Acknowledgments: The authors acknowledge the assistance of Javier Marfil (Eurecat) with the HPDC trials, Marc Soler (Eurecat) with the analysis of the chemical composition by EOS. The authors acknowledge as well Raffmetal, ASAS and Profilglass, SALEMA project partners, for supplying the alloys used for the HPDC, extrusion and stamping studies, respectively.

Conflicts of Interest: The authors declare no conflict of interest.

References

1. European Aluminium. Available online: https://european-aluminium.eu/wp-content/uploads/2022/10/aluminum-content-in-european-cars_european-aluminium_public-summary_101019-1.pdf (accessed on 23 May 2023).
2. A. Ismail, M.S. Mohamed. Review on sheet metal forming process of aluminium alloys. In Proceedings of the 17 MS 129th Int. AMME Conference, 19-21 April 2016
3. Miller, W.S.; Zhuang, L.; Bottema, J.; Wittebrood, A.J.; De Smet, P.; Haszler, A.; Vieregge A. Recent development in aluminium alloys for the automotive industry. *Mater. Sci. and Eng. A* **2000**, *280*, 37-49.
4. Graedel, T.E.; Allwood, J.; Birat, J.-P.; Buchert, M.; Hagelüken, C.; Reck, B.K.; Sibley, S.F. Guido Sonnemann: What do We Know about Metal Recycling Rates? *J. Ind. Ecology* **2011** *15*(3), 355-366, <https://doi.org/10.1111/j.1530-9290.2011.00342.x>
5. Kaufmann, H. Science of dirty alloys, *AluReport* **2019**, *2*, 22-23.
6. Jaradeh, M.; Carlberg, T. Method Developed for Quantitative Analysis of Inclusions in Solidified Aluminum Ingots. *Metall. Mater. Trans. B* **2011**, *42*, 121-132, Doi: 10.1007/s11663-010-9463-4
7. Raabe, D.; Ponge, D. Making sustainable aluminum by recycling scrap: The science of “dirty” alloys. *Prog. Mater. Sci.* **2022**, *128*, 100947
8. Samuel, A.M.; Samuel, F.H. Metallurgical aspects of inclusion assessment in Al–6%Si casting alloy using the LIMCA technique. *Int. J. Met.* **2018**, *12*(3), 643-657
9. Pana, M.A.; Moldovan, P. Researches Concerning PoDFA Method for 5083 Alloys. In Proceedings of the 12th International Conference on Aluminium Alloys, Yokohama, Japan, 5-9 September 2010
10. Prillhofer, B.; Antrekowitsch, H.; Böttcher, H.; Enright P. Nonmetallic inclusions in the secondary aluminum industry for the Production of aerospace alloys. In Proceedings of TMS. Light Metals, 2008
11. Boczkal, S.; Augustyn, B.; Hrabia-Wiśnios, J.; Kapinos, D.; Lewis, G.; Bareel, P.-F.; Savelli, S.; da Silva, M.; Özen, T. Preparation of High-Quality 6xxx Aluminium Eco Alloys Cast in Billets. *Eng. Proc.* **2023**, *43*, 23. <https://doi.org/10.3390/engproc2023043023>
12. De Caro, D.; Tedesco, M.M.; Pujante, J.; Bongiovanni, A.; Sbrega, G.; Bricco, M.; Rizzo, P. Effect of Recycling on the Mechanical Properties of 6000 Series Aluminum-Alloy Sheet. *Mater.* **2023**, *16*(20), 6778; <https://doi.org/10.3390/ma16206778>
13. Scamans, G.; Li, H.T.; Fan, Z; (2012). Melt Conditioned Casting of Aluminum Alloys. In Proceedings of the ICAA13, 3-7 June 2012, https://doi.org/10.1007/978-3-319-48761-8_213
14. Smith, N.; Kvithyld, A; Tranell, G. The Mechanism Behind the Oxidation Protection of High Mg Al Alloys with Beryllium. *Metall Mater Trans B* **2018**, *49*, 2846–2857. <https://doi.org/10.1007/s11663-018-1340-6>
15. Cao, X.; Campbell; J. Oxide inclusion defects in Al-Si-Mg cast alloys. *Can. Metall. Q.*, **2005**, *44*, 435-448
16. Vonica, D.; Moldovan, P.; Stănică, C.; Buțu, M.; Ciurdaș, M.; Pană, M. Investigations of the nature of non-metallic inclusions in Al-Mg-Mn alloys. *U.P.B. Sci. Bull., Series B* **2013**, *75* (4), ISSN 14546 – 3540

17. Baquedano, A.; Niklas, A.; Fernández-Calvo, A.I.; Plata, G.; Lozares, J.; Berlanga-Labari, C. Comparative Study of the Metallurgical Quality of Primary and Secondary AlSi10MnMg Aluminium Alloys, *Met.* **2021**, *11*, 1147. <https://doi.org/10.3390/met11071147>
18. Stanică, C.; Moldovan, P. Aluminum melt cleanliness performance evaluation using PoDFA (porous disk filtration apparatus) technology *U.P.B. Sci. Bull. B: Chem. Mater. Sci.* **2009**, *71*
19. Ásbjörnsson, Einar. Dispersion of grain refiner particles in molten aluminium. *PhD Thesis, Univ. of Nottingham* **2001**
20. Aluminium And Its Alloys – Fluidity Evaluation Via Multi Strip Testing Moulds. *CEN-CENELEC Workshop Agreements* **2024**
21. Snopinski, P.; Tanski, T.; Gołombek, K.; Ruzs, S.; Hilser, O.; Donic, T.; Nuckowski, P.M.; Benedyk, M. Strengthening of AA5754 Aluminum Alloy by DRECE Process Followed by Annealing Response Investigation: *Mater.* **2020**, *13*, 301; doi:10.3390/ma13020301
22. Dou, K.; Lordan, E.; Zhang, Y.; Jacot, A.; Fan, Z. A novel approach to optimize mechanical properties for aluminium alloy in High pressure die casting (HPDC) process combining experiment and modelling. *J. Mater. Process. Technol.* **2021**, *296*, 117193; <https://doi.org/10.1016/j.jmatprotec.2021.117193>
23. Akhtar, S.; Molina, R.; Di Sabatino, M.; Arnberg, L. On the quality of A354 ingots and its impact on cast product. *Metall. Sci. Technol.* **2009**, *27*, 2-10
24. Jaradeh, M.M.; Carlberg, T. Method Developed for Quantitative Analysis of Inclusions in Solidified Aluminum Ingots. *Metall. Mater. Trans. B* **2011**, *42*, 121–132. <https://doi.org/10.1007/s11663-010-9463-4>
25. Yang, J.; Bao, S.; Akhtar, S.; Tundal, U.; Tjÿtta, S.; Li, Y. The Influences of Grain Refiner, Inclusion Level, and Filter Grade on the Filtration Performance of Aluminium Melt. *Metall. Mater. Trans. B*, **2021**, *52*, 3946-3960; <https://doi.org/10.1007/s11663-021-02310-7>
26. Detomi, A.M.; Messias, A.J.; Majer, S.; Cooper, P.S. The impact of TiAl and TiAl Grain Refiners on Cast house Processing, In Proceedings of TMS. Light Metals, New Orleans, LA, 2001, 919-925
27. Kvithyld, A.; Meskers, C.E.M.; Gaal, S. et al. Recycling light metals: Optimal thermal de-coating. *JOM* **2008**, *60*, 47–51. <https://doi.org/10.1007/s11837-008-0107-y>

Disclaimer/Publisher’s Note: The statements, opinions and data contained in all publications are solely those of the individual author(s) and contributor(s) and not of MDPI and/or the editor(s). MDPI and/or the editor(s) disclaim responsibility for any injury to people or property resulting from any ideas, methods, instructions or products referred to in the content.